IEEE TRANSACTIONS ON

SIGNAL PROCESSING

A PUBLICATION OF THE IEEE SIGNAL PROCESSING SOCIETY

www.ieee.org/sp/index.html

APRIL 2001 VOLUME 49 NUMBER 4 ITPRED (ISSN 1053–587X)

PAPERS

(Contents Continued on Back Cover)

Linear Prediction Approach to Direction Estimation of Cyclostationary Signals in Multipath Environment

Jingmin Xin, *Member, IEEE*, and Akira Sano, *Member, IEEE*

***Abstract*—In this paper, we investigate the estimation of the directions-of-arrival (DOA) of closely spaced narrowband cyclostationary signals in the presence of multipath propagation. By exploiting the spatial and temporal properties of most communication signals, we propose a new cyclic forward-backward linear prediction (FBLP) approach for coherent signals impinging on a uniform linear array (ULA). In the proposed algorithm, the evaluation of the cyclic array covariance matrix is avoided, and the difficulty of choosing the optimal time lag parameter is alleviated. As a result, the proposed approach has two advantages: 1) The computational load is relatively reduced, and 2) the robustness of estimation is significantly improved. The performance of the proposed approach is confirmed through numerical examples, and it is shown that this approach is superior in resolving the closely spaced coherent signals with a small length of array data and at relatively low signal-to-noise ratio (SNR).**

***Index Terms*—Array signal processing, cyclostationarity, directions-of-arrival estimation, linear prediction, singular value decomposition, spatial smoothing.**

I. Introduction

In ARRAY signal processing, a major problem is the estimation of the directions-of-arrival (DOA) of the signals impinging on an array of sensors. For estimating the directions of multiple narrowband signals from the noisy array data, maximum likelihood (ML) methods and subspace-based methods are well known. While subspace-based methods such as MUSIC [1], ESPRIT [2], minimum-norm [3], and MODE [in a uniform linear array (ULA) case] [6], [41] are more computationally efficient than the ML methods [4]–[7], all of them except MODE are unsuitable for coherent signals. To tackle the problem of coherent signals, several modifications to the subspace-based methods have been proposed [8]–[12]; among them, spatial smoothing (SS) [8] is a popular preprocessing scheme. MODE is also known to be statistically efficient in cases when either the number of snapshots or the signal-to-noise ratio (SNR) is sufficiently large [6], [48], [49]. However, in array processing of wireless communication systems, there are some practical situations where the overall number of incident signals is greater than the number of sensors, even though the number of desired signals is smaller, and multipath propagation due to various reflections is often encountered. Furthermore, the number of snapshots is usually limited. In these scenarios, the performance of most subspace-based methods and their variants will degrade. Moreover, the subspace-based methods basically rely on the spatial information contained in the received data, whereas the temporal properties of the desired incident signals are ignored.

Most man-made communication signals exhibit cyclostationarity for a given cycle frequency because of the underlying periodicity arising from carrier frequencies or baud rates [13], [14]. Many direction estimation methods exploiting this inherently temporal property have been developed recently (see, e.g., [14]–[21] and references therein) in which the stationary noise and the interfering signals that do not share a cycle frequency common to the desired signals are suppressed. For estimating the directions of coherent cyclostationary signals, a cyclic ML method [22] and an SS-based cyclic MUSIC method [23], [50] were proposed. However, the former is computationally expensive because it involves a multidimensional optimization, whereas the latter is still not computationally efficient enough since the cyclic correlation matrices of subarrays must be evaluated.

Therefore, this paper aims to investigate an efficient method for estimating the DOA of closely spaced narrowband cyclostationary signals in a multipath propagation environment. The linear prediction (LP) methods are attractive for resolving the closely spaced signals with small length of data and at low SNR because of their computational simplicity [24]–[26]. In this paper, we propose a new cyclic forward-backward LP (FBLP) approach to localizing the coherent signals impinging on a ULA. By utilizing the spatial and temporal properties of the incoming signals, a modified FBLP equation is formed with a subarray scheme, and then, the prediction coefficients determined from a cyclic LP equation can be used to estimate the DOA of the coherent signals. As the cyclic correlation function is dependent on the time lag parameter, the choice of the optimal lag is crucial for the cyclic methods [15], [17], [18], [20], but it is rarely available. In this paper, we use multiple lags in a forward-backward way to exploit the cyclic statistical information efficiently. In addition, the choice of the subarray size (i.e., the order of the LP model plus one) is important to achieve the best performance of DOA estimation. For sufficiently high SNR, an analytical expression of error variance of spectral peak position is derived using linear approximation. Then, the optimal subarray size minimizing the peak position variance is clarified. Unlike the SS-based cyclic MUSIC method [23], [50], the proposed approach avoids evaluating the cyclic array covariance matrix. Thus, it is more capable of discriminating in favor of the desired coherent signals against the noise and interfering signals than the conventional LP-based methods [9], [11], and its computation is simpler than that of the

Manuscript received January 17, 2000; revised September 6, 2000. This work was presented in part at the IFAC 14th World Congress, Beijing, China, July 1999. The associate editor coordinating the review of this paper and approving it for publication was Prof. Jian Li.

J. Xin is with YRP Mobile Telecommunications Key Technology Research Laboratories Co., Ltd., Yokosuka, Japan (e-mail: xin@yrp-ktrl.co.jp).

A. Sano is with Department of System Design Engineering, Keio University, Yokohama, Japan (e-mail: sano@sd.keio.ac.jp).

Publisher Item Identifier S 1053-587X(01)02239-5.

SS-based cyclic MUSIC method. The performance of the proposed approach is verified through numerical examples.

II. Problem Formulation

A. Data Model

We consider a ULA of M identical and omnidirectional sensors with spacing d and assume that p narrowband signals $\{s_k(n)\}$ with zero-mean and center frequency f_c are far enough away and come from distinct directions $\{\theta_k\}$. The received signal $y_i(n)$ at the ith sensor can be expressed by

$$y_i(n) = x_i(n) + w_i(n) \tag{1}$$

$$x_i(n) = \sum_{k=1}^{p} s_k(n)\, e^{j\omega_0 (i-1)\tau_k(\theta)} \tag{2}$$

where $x_i(n)$ is the noiseless received signal, $w_i(n)$ is the additive noise, $\omega_0 = 2\pi f_c$, $\tau_k(\theta) = (d/c)\sin\theta_k$, c is the speed of propagation, and θ_k is the measured relatively to the normal of the array.

From (1) and (2), the received array data can be rewritten in a more compact form as

$$\boldsymbol{y}(n) = \boldsymbol{A}\boldsymbol{s}(n) + \boldsymbol{w}(n) \tag{3}$$

where $\boldsymbol{y}(n) = [y_1(n), y_2(n), \cdots, y_M(n)]^T$, $\boldsymbol{s}(n) = [s_1(n), s_2(n), \cdots, s_p(n)]^T$, $\boldsymbol{w}(n) = [w_1(n), w_2(n), \cdots, w_M(n)]^T$, $\boldsymbol{A} = [\boldsymbol{a}(\theta_1), \boldsymbol{a}(\theta_2), \cdots, \boldsymbol{a}(\theta_p)]$, $\boldsymbol{a}(\theta_k) = [1, e^{j\omega_0\tau_k(\theta)}, \cdots, e^{j\omega_0(M-1)\tau_k(\theta)}]^T$, and $(\cdot)^T$ denotes transpose.

We will consider the direction estimation under the following assumptions on the data model.

A1) The array steering matrix $\boldsymbol{A}$ is unambiguous, i.e., the steering vectors $\{\boldsymbol{a}(\theta_1), \boldsymbol{a}(\theta_2), \cdots, \boldsymbol{a}(\theta_p)\}$ are linearly independent for any set of distinct $\{\theta_1, \theta_2, \cdots, \theta_p\}$.

A2) There is frequency-flat multipath propagation [8], [28]. Without loss of generality, the first q ($1 \le q \le p$ and $q < 2M/3$ [see Remark C)] signals are coherent ones from the desired source that are expressed by

$$s_k(n) = \beta_k s_1(n) \tag{4}$$

where β_k is the multipath coefficient that represents the complex attenuation of the kth signal with respect to the first one $s_1(n)$ with $\beta_k \neq 0$ and $\beta_1 = 1$.

A3) The desired source exhibits the second-order cyclostationarity with the cycle frequency α, and it is cyclically uncorrelated with the other signals for this cycle frequency.

A4) The noises $\{w_i(n)\}$ are cyclically uncorrelated with themselves and with the incident signals at the considered cycle frequency α.

A5) The number of coherent signals q and the cycle frequency α are known.

Remark A: When the number of coherent signals is unknown, it can be estimated by using the methods presented in [14, ch. 3] and [16]. We have also proposed a detection method by minimizing the mean-squared-error (MSE) of the estimated LP parameters in [21] and [46], and it is well suited to be used in conjunction with the approach for the coherent signals described in this paper. If the cycle frequency α is unknown, it can be estimated from the finite data by using the methods proposed in [18] and [29].

B. Linear Prediction with Subarrays

Here, we consider the case that the interfering signals are absent. The noiseless received signals $\{x_i(n)\}$ in (2) differ only by a phase factor $\omega_0\tau_k(\theta)$; therefore, from Prony's method [30], we can find that the noiseless signals $\{x_i(n)\}$ obey a linear difference equation [9], [24]. By dividing the array into L overlapping subarrays of size m, where $L = M - m + 1$ and $m \ge q + 1$, i.e., the lth forward subarray comprises sensors $\{l, l+1, \cdots, l+m-1\}$, the signal $x_{l+m-1}(n)$ can be exactly predicted by $x_l(n), x_{l+1}(n), \cdots, x_{l+m-2}(n)$ as [24], [30]

$$x_{l+m-1}(n) = \boldsymbol{x}_{f,l}^T(n)\,\boldsymbol{a} \tag{5}$$

where $\boldsymbol{x}_{f,l}(n) = [x_l(n), x_{l+1}(n), \cdots, x_{l+m-2}(n)]^T$, $\boldsymbol{a} = [a_{m-1}, a_{m-2}, \cdots, a_1]^T$, and $\{a_i\}$ are the LP coefficients. Similarly, by partitioning the full array into L subarrays with m sensors in the backward direction, we obtain the LP equation for the lth backward subarray as [9]

$$x_{L-l+1}^*(n) = \boldsymbol{x}_{b,l}^T(n)\,\boldsymbol{a} \tag{6}$$

where $\boldsymbol{x}_{b,l}(n) = [x_{M-l+1}^*(n), x_{M-l}^*(n), \cdots, x_{L-l+2}^*(n)]^T$, and the asterisk denotes the complex conjugate.

From (1), (5), and (6), we then get the following forward LP (FLP) and backward LP (BLP) models for the noisy received data

$$y_{l+m-1}(n) = \boldsymbol{y}_{f,l}^T(n)\,\boldsymbol{a} + \varepsilon_{f,l}(n) \tag{7}$$

$$y_{L-l+1}^*(n) = \boldsymbol{y}_{b,l}^T(n)\,\boldsymbol{a} + \varepsilon_{b,l}(n) \tag{8}$$

where $\boldsymbol{y}_{f,l}(n) = [y_l(n), y_{l+1}(n), \cdots, y_{l+m-2}(n)]^T$, $\boldsymbol{y}_{b,l}(n) = [y_{M-l+1}^*(n), y_{M-l}^*(n), \cdots, y_{L-l+2}^*(n)]^T$, $\varepsilon_{f,l}(n)$ and $\varepsilon_{b,l}(n)$ are the forward and backward prediction errors given by $\varepsilon_{f,l}(n) = w_{l+m-1}(n) - \boldsymbol{w}_{f,l}^T(n)\,\boldsymbol{a}$, $\varepsilon_{b,l}(n) = w_{L-l+1}^*(n) - \boldsymbol{w}_{b,l}^T(n)\,\boldsymbol{a}$, $\boldsymbol{w}_{f,l}(n) = [w_l(n), w_{l+1}(n) \cdots, w_{l+m-2}(n)]^T$, $\boldsymbol{w}_{b,l}(n) = [w_{M-l+1}^*(n), w_{M-l}^*(n), dots, w_{L-l+2}^*(n)]^T$.

In the LP-based DOA estimation methods, the estimation of the LP coefficients is very important [31]. The accumulation of the additive noises in $y_{l+m-1}(n)$, $y_{L-l+1}^*(n)$, $\boldsymbol{y}_{f,l}(n)$, and $\boldsymbol{y}_{b,l}(n)$ will cause the ordinary least squares (LS) or minimum-norm estimate from (7) and (8) to become biased and inconsistent [32], and this estimate will make the DOA estimation unreliable. The total least squares (TLS) LP [33] and the smoothed LP [11] methods can be applied to reduce the noise effect, but their performances deteriorate when the total number of incoming signals exceeds the number of sensors, even though the number of desired signals is smaller. In this paper, we will exploit the inherent cyclostationarity of most communication signals to suppress the interfering signals and noise.

III. Cyclic DOA Estimation of Coherent Signals

A. Cyclic Correlation of Noisy Data

First, the noiseless signal $x_i(n)$ in (2) can be rewritten compactly as

$$x_i(n) = \boldsymbol{b}_i^T(\theta)\boldsymbol{s}(n) = \boldsymbol{s}^T(n)\boldsymbol{b}_i(\theta) \tag{9}$$

where $\boldsymbol{b}_i(\theta) = [e^{j\omega_0(i-1)\tau_1(\theta)}, e^{j\omega_0(i-1)\tau_2(\theta)}, \cdots, ^{j\omega_0(i-1)\tau_p(\theta)}]^T$. Then, from the definition of the cyclic correlation function [13], [14] and under the assumptions regarding the source signals and additive noises, we obtain the cyclic correlation function $r^{\alpha}_{y_i, y_k}(\tau)$ between the noisy signals $y_i(n)$ and $y_k(n)$ as

$$\begin{aligned} r^{\alpha}_{y_i, y_k}(\tau) &= \langle y_i(n) y_k^*(n+\tau) e^{-j2\pi\alpha n} \rangle \\ &= \boldsymbol{b}_i^T(\theta) \boldsymbol{R}_s^{\alpha}(\tau) \boldsymbol{b}_k^*(\theta) \end{aligned} \tag{10}$$

where $\langle z(n) \rangle = \lim_{N\to\infty} (1/N) \sum_{n=0}^{N-1} z(n)$ denotes the time average of $z(n)$, τ is the lag parameter, and $\boldsymbol{R}_s^{\alpha}(\tau)$ is the cyclic covariance matrix of the source signals given by

$$\boldsymbol{R}_s^{\alpha}(\tau) = \langle \boldsymbol{s}(n) \boldsymbol{s}^H(n+\tau) e^{-j2\pi\alpha n} \rangle \tag{11}$$

where $(\cdot)^H$ denotes the Hermitian transpose. Clearly, the affections of the arbitrary (not necessarily stationary and/or spatially white) noise and interference vanish if the cycle frequency α is appropriately selected; therefore, the signal detection capability can be improved.

However, because of the coherency of the q signals from the desired source, the cyclic covariance matrix of source signals $\boldsymbol{R}_s^{\alpha}(\tau)$ in (11) is obtained as

$$\begin{aligned} \boldsymbol{R}_s^{\alpha}(\tau) &= \langle \boldsymbol{\beta}\, s_1(n) \boldsymbol{\beta}^H s_1^*(n+\tau) e^{-j2\pi\alpha n} \rangle \\ &= r_s^{\alpha}(\tau)\, \boldsymbol{\beta}\boldsymbol{\beta}^H \end{aligned} \tag{12}$$

where $\boldsymbol{\beta}$ is the vector of multipath coefficients given by $\boldsymbol{\beta} = [\beta_1, \cdots, \beta_q, \beta_{q+1}, \cdots, \beta_p]^T$ with $\beta_{q+1} = \cdots = \beta_p = 0$, β_k is defined in (4) for $k = 1, 2, \cdots, q$, and $r_s^{\alpha}(\tau)$ is the cyclic autocorrelation function of the signal $s_1(n)$ given by $r_s^{\alpha}(\tau) = \langle s_1(n)\, s_1^*(n+\tau) e^{-j2\pi\alpha n} \rangle$. We can easily find that the cyclic matrix $\boldsymbol{R}_s^{\alpha}(\tau)$ is singular, i.e., rank$(\boldsymbol{R}_s^{\alpha}(\tau)) = 1$, and it brings degradation to the ordinary cyclic methods.

B. Linear Prediction Approach to DOA Estimation

In the absence of interfering signals, from (10), (1) and (7), we obtain the cyclic correlation $r^{\alpha}_{y_{l+m-1}, y_M}(\tau)$ between the noisy signal $y_{l+m-1}(n)$ in the lth forward subarray and the signal $y_M(n)$ as

$$\begin{aligned} r^{\alpha}_{y_{l+m-1}, y_M}(\tau) &= \langle y_{l+m-1}(n) y_M^*(n+\tau) e^{-j2\pi\alpha n} \rangle \\ &= \langle \boldsymbol{y}^T_{f, l}(n) y_M^*(n+\tau) e^{-j2\pi\alpha n} \rangle \boldsymbol{a} \\ &= \boldsymbol{\varphi}^T_{f, l}(\tau) \boldsymbol{a} \end{aligned} \tag{13}$$

where $\boldsymbol{\varphi}_{f, l}(\tau) = [r^{\alpha}_{y_l, y_M}(\tau), r^{\alpha}_{y_{l+1}, y_M}(\tau), \cdots, r^{\alpha}_{y_{l+m-2}, y_M}(\tau)]^T$. Equivalently, we can obtain the cyclic correlation $r^{\alpha}_{y_1, y_{L-l+1}}(\tau)$ between the noisy signal $y_1(n)$ and the signal $y_{L-l+1}(n)$ in the lth backward subarray as

$$\begin{aligned} r^{\alpha}_{y_1, y_{L-l+1}}(\tau) &= \langle y_1(n) y^*_{L-l+1}(n+\tau) e^{-j2\pi\alpha n} \rangle \\ &= \langle y_1(n) \boldsymbol{y}^T_{b, l}(n+\tau) e^{-j2\pi\alpha n} \rangle \boldsymbol{a} \\ &= \boldsymbol{\varphi}^T_{b, l}(\tau) \boldsymbol{a} \end{aligned} \tag{14}$$

where $\boldsymbol{\varphi}_{b, l}(\tau) = [r^{\alpha}_{y_1, y_{M-l+1}}(\tau), r^{\alpha}_{y_1, y_{M-l}}(\tau), \cdots, r^{\alpha}_{y_1, y_{L-l+2}}(\tau)]^T$. As shown in (10)–(12), even in the presence of interfering signals, the affections of the interfering signals and noise are eliminated by exploiting the cyclostationarity. We can find that the prediction relations (13) and (14) in the cyclic domain are valid when the interfering signals are present. Now, we consider the DOA estimation of the desired coherent cyclostationary signals by utilizing the LP technique.

By letting $l = 1$ to L and combining (13) and (14), we can obtain an FBLP equation for the cyclic correlations as

$$\boldsymbol{z}(\tau) = \boldsymbol{\Phi}(\tau)\, \boldsymbol{a} \tag{15}$$

where $\boldsymbol{z}(\tau) = [\boldsymbol{z}_f^T(\tau), \boldsymbol{z}_b^T(\tau)]^T$, $\boldsymbol{\Phi}(\tau) = [\boldsymbol{\Phi}_f^T(\tau), \boldsymbol{\Phi}_b^T(\tau)]^T$, $\boldsymbol{z}_f(\tau) = [r^{\alpha}_{y_m, y_M}(\tau), r^{\alpha}_{y_{m+1}, y_M}(\tau), \cdots, r^{\alpha}_{y_M, y_M}(\tau)]^T$, $\boldsymbol{z}_b(\tau) = [r^{\alpha}_{y_1, y_{M-m+1}}(\tau), r^{\alpha}_{y_1, y_{M-m}}(\tau), \cdots, r^{\alpha}_{y_1, y_1}(\tau)]^T$, $\boldsymbol{\Phi}_f(\tau) = [\boldsymbol{\varphi}_{f, 1}(\tau), \boldsymbol{\varphi}_{f, 2}(\tau), \cdots, \boldsymbol{\varphi}_{f, L}(\tau)]^T$, and $\boldsymbol{\Phi}_b(\tau) = [\boldsymbol{\varphi}_{b, 1}(\tau), \boldsymbol{\varphi}_{b, 2}(\tau), \cdots, \boldsymbol{\varphi}_{b, L}(\tau)]^T$. To combat the rank deficiency resulting from signal coherency, we have the following proposition.

Proposition: If the array is partitioned properly to ensure $2L \geq q$, the rank of the cyclic matrix $\boldsymbol{\Phi}(\tau)$ in (15) equals the number of the desired coherent signals.

Proof: See Appendix A. ■

We can find that the dimension of signal subspace is restored to q as long as the total number of subarrays is at least q; therefore, it is possible to estimate the directions of the desired coherent signals from (15) without any influence from additive noise or interfering signals. However, the $2L \times (m-1)$ matrix $\boldsymbol{\Phi}(\tau)$ in (15) is usually rank-deficient due to $q \leq 2L$ and $q \leq m-1$. Hence, the ordinary LS estimate of the parameter $\boldsymbol{a}$ from (15) will be numerically unstable [38]; this ill-conditioning can adversely affect the performance of direction estimation [31]. Hence, we use the truncated singular value decomposition (SVD) to obtain a numerically reliable estimation, where the q principal singular values and the corresponding singular vectors of the matrix $\boldsymbol{\Phi}(\tau)$ are used [9], [24], [31], [35], [36].

By performing the SVD on the matrix $\boldsymbol{\Phi}(\tau)$ in (15), we obtain

$$\boldsymbol{\Phi}(\tau) = \boldsymbol{U}\boldsymbol{\Lambda}\boldsymbol{V}^H \tag{16}$$

where $\boldsymbol{U}$ and $\boldsymbol{V}$ are the unitary matrices given by $\boldsymbol{U} = [\boldsymbol{u}_1, \boldsymbol{u}_2, \cdots, \boldsymbol{u}_{2L}]$ and $\boldsymbol{V} = [\boldsymbol{v}_1, \boldsymbol{v}_2, \cdots, \boldsymbol{v}_{m-1}]$, $\boldsymbol{\Lambda}$ is the diagonal matrix given by $\boldsymbol{\Lambda} = \text{diag}(\lambda_1, \lambda_2, \cdots, \lambda_{\min(2L, m-1)})$ with $\lambda_1 \geq \cdots \geq \lambda_q > \lambda_{q+1} = \cdots = \lambda_{\min(2L, m-1)} = 0$, $\{\lambda_i\}$ are the singular values, and $\{\boldsymbol{u}_i\}$ and $\{\boldsymbol{v}_i\}$ are the corresponding right and left singular vectors. Then, the minimum-norm estimate of the LP parameter $\boldsymbol{a}$ is obtained [24], [35]

$$\hat{\boldsymbol{a}} = \sum_{i=1}^{q} \frac{\boldsymbol{u}_i^H \boldsymbol{z}(\tau)}{\lambda_i} \boldsymbol{v}_i. \tag{17}$$

Finally, by finding the phase of the q zeros of the polynomial $D(z) = 1 - \hat{a}_1 z^{-1} - \hat{a}_2 z^{-2} - \cdots - \hat{a}_{m-1} z^{-(m-1)}$ closest to the unit circle in the z-plane, or by searching for the q highest peaks of the spectrum $1/|D(e^{j\omega_0 (d/c) \sin\theta})|^2$, the directions of the desired coherent signals can be estimated [3], [24], [30].

C. Cyclic Localization Algorithm

As the cyclic correlation function is dependent on the lag parameter τ [13], [14], if the cyclic correlation of one source is zero or insignificant for a given τ, then this signal will not be resolved. The choice of the optimal lag parameter is important in cyclic methods [15], [17], [18], [20], but it is rarely available. To combat this problem, some methods were suggested [15], [17], [27]. In the SS-based cyclic MUSIC method [23], [50], the spatially smoothed cyclic correlation matrices corresponding to the lags $\tau = -Q, \cdots, -1, 0, 1, \cdots, Q$ were averaged and then used to estimate the directions of coherent signals, where Q is a positive integer. However, this method is not computationally efficient enough because the cyclic correlation matrices of subarrays must be evaluated.

In order to alleviate the difficulty in choosing the optimal lag and to exploit the cyclic statistics effectively, we use multiple lags to obtain a robust estimate of the LP parameter $\boldsymbol{a}$. By concatenating (15) for $\tau = -Q, \cdots, -1, 0, 1, \cdots, Q$, we can obtain a modified cyclic vector-matrix form as

$$\boldsymbol{z} = \boldsymbol{\Phi}\,\boldsymbol{a} \tag{18}$$

where $\boldsymbol{z} = [\boldsymbol{z}^T(-Q), \cdots, \boldsymbol{z}^T(-1), \boldsymbol{z}^T(0), \boldsymbol{z}^T(1), \cdots, \boldsymbol{z}^T(Q)]^T$, and $\boldsymbol{\Phi} = [\boldsymbol{\Phi}^T(-Q), \cdots, \boldsymbol{\Phi}^T(-1), \boldsymbol{\Phi}^T(0), \boldsymbol{\Phi}^T(1), \cdots, \boldsymbol{\Phi}^T(Q)]^T$. Then, on the above derivations, we can estimate the directions of the desired coherent signals with the cycle frequency α from (18).

In summary, the proposed FBLP-based algorithm for estimating the DOA of coherent cyclostationary signals from the finite array data $\{y_1(n), y_2(n), \cdots, y_M(n)\}_{n=0}^{N-1}$ is as follows.

1) Set the subarray size m to satisfy $m \geq q+1$ and $2L \geq q$, where $L = M - m + 1$.
2) Calculate the estimates of the cyclic correlation functions $r^{\alpha}_{y_i,y_M}(\tau)$ and $r^{\alpha}_{y_1,y_k}(\tau)$ from the finite N received signals $\{\boldsymbol{y}(n)\}$ for $\tau = -Q, \cdots, -1, 0, 1, \cdots, Q$ as

$$\hat{r}^{\alpha}_{y_i,y_k}(\tau) = \frac{1}{N}\sum_{n=0}^{N-1-\tau} y_i(n) y_k^*(n+\tau) e^{-j2\pi\alpha n} \quad \text{for } \tau \geq 0 \tag{19}$$

$$\hat{r}^{\alpha}_{y_i,y_k}(\tau) = \frac{1}{N}\sum_{n=-\tau}^{N-1} y_i(n) y_k^*(n+\tau) e^{-j2\pi\alpha n} \quad \text{for } \tau < 0 \tag{20}$$

where $i = 1, 2, \cdots, M$ and $k = M$ for $r^{\alpha}_{y_i,y_M}(\tau)$, whereas $k = 1, 2, \cdots, M$ and $i = 1$ for $r^{\alpha}_{y_1,y_k}(\tau)$.
3) Form the estimated cyclic vector $\hat{\boldsymbol{z}}$ and matrix $\hat{\boldsymbol{\Phi}}$ as (18) by using (19), (20), and (15).
4) Perform the SVD on the estimated matrix $\hat{\boldsymbol{\Phi}}$ as (16), where L is replaced by $\overline{L} = (2Q+1)L$.
5) Calculate the minimum-norm estimate of the LP parameter $\boldsymbol{a}$ as

$$\hat{\boldsymbol{a}} = \sum_{i=1}^{q} \frac{\hat{\boldsymbol{u}}_i^H \hat{\boldsymbol{z}}}{\hat{\lambda}_i} \hat{\boldsymbol{v}}_i. \tag{21}$$

6) Estimate the DOA of the coherent signals from the q highest peak locations of the spectrum given by $1/|\hat{D}(e^{j\omega_0 (d/c)\sin\theta})|^2$.

Remark B: We find that the proposed cyclic FBLP-based approach involves the computation of the $2N_\tau M$ cyclic correlations of the sensor signals to form the cyclic matrix $\boldsymbol{\Phi}$ in (18), i.e., it requires $O(2N_\tau M)$ operations, whereas the cyclic MUSIC algorithms [23], [50] based on the SS [8] and improved SS [37] require $O(N_\tau(M + (m-1)(2M-m)))$ and $O(N_\tau M^2)$ operations for the evaluation of the cyclic matrices, respectively, where N_τ is the total number of time lags. Obviously, in this paper, the computational load in decorrelation step is reduced by $2/(1+(m-1)(2-m/M))$ or $2/M$ times, respectively, because the evaluation of the cyclic array covariance matrix can be avoided.

The implementation of the proposed approach requires two major steps: i) computation of the cyclic correlations to form $\hat{\boldsymbol{z}}$ and $\hat{\boldsymbol{\Phi}}$ and ii) estimation of LP parameter $\boldsymbol{a}$ by SVD. Calculating the cyclic correlations for multiple lags takes approximately $52N_\tau NM$ flops, where a flop is defined as a floating-point addition or multiplication operation as adopted by MATLAB software. The number of flops needed by the SVD of matrix $\hat{\boldsymbol{\Phi}}$ is of the order $O((2LN_\tau)^2(m-1))$, whereas the computation of $\hat{\boldsymbol{a}}$ requires $8(m-1)(q^2 + 2LN_\tau q + 2LN_\tau) + q$ flops. Thus, a rough estimate of the number of MATLAB flops required by the proposed approach is $52N_\tau NM$ when $N \gg M$, where the computations needed by the remaining steps are negligible.

Remark C: For estimating the directions of the q coherent signals, as stated in the Proposition, the number of forward and backward subarrays must be at least q, i.e., $2L \geq q$, and the size m of each subarray must be greater than q, where $L = M - m + 1$. It follows that $2(M - m + 1) \geq q$ and $m \geq q + 1$, i.e., the minimum number of sensors needed in the array must be at least $M \geq 3q/2$ (it follows that the maximum number of the coherent signals will be $q \leq 2M/3$ for M sensors). Equivalently, the subarray size m (i.e., the order of the prediction model plus one) must be chosen to satisfy the inequality $q + 1 \leq m \leq M - q/2 + 1$. To improve the estimation performance, m should be chosen as large as possible in order to increase the effective aperture. However, for a very large value of m, fewer element terms of $\boldsymbol{\Phi}(\tau)$ [equal to $2(M - m + 1)$ in number] are formed to compute the singular values and singular vectors of $\boldsymbol{\Phi}(\tau)$ (and $\boldsymbol{\Phi}$). This results in larger perturbations of the singular values and singular vectors so that the resolution capability decreases despite the increased aperture [9], [24]. The choice of the optimal value of m is crucial to achieve the best performance of direction estimation. A compromise value of the subarray size should be determined by balancing the effects of resolution and stability [9], [24]; we experimentally determine it to be about $M/3 + 1$ for high SNR. More details can be found in Section III-D.

Remark D: In practice, the cyclic correlation function has to be evaluated from the array data with a finite number of snapshots N, and estimation perturbation is unavoidable. If Q is very large, the disturbances due to the finite number of snapshots may have a relatively large influence, and the effect of additive noise will be included. On the other hand, if it is very small, the effect of multiple lags may be neglected because very little information about the cyclic correlation characteristics is contained. As a result, Q should be determined by a tradeoff. In this paper, we choose Q large enough so that $\hat{r}^{\alpha}_{y_i,y_i}(\tau)$ are nonzero and significantly varying for $|\tau| > Q$ [17]. The statistical test [29] can be used to select a statistically significant value of Q.

D. Optimal Subarray Size

The optimal subarray size (i.e., the optimal order of LP model plus one) is desired to obtain the best estimation performance, but it generally depends on the number of desired coherent signals, the SNR, and the angle separation of incident signals. In the proposed approach, the directions are determined from the peak positions of the spectrum $1/D(e^{j\omega_0 (d/c)\sin\theta})|^2$. Here, we investigate the choice of the subarray size to minimize the variance of peak position error.

The derivation of the error variance of spectral peak position for direction estimation is tedious, so here, we sketch the derivation for the FLP method when the SNR is sufficiently high. As the interfering signals are suppressed in the proposed approach, for notational simplicity, we assume that the interfering signals are absent and that the noises are temporally and spatially uncorrelated white complex Gaussian noises, i.e., $p = q$, $\beta_k \neq 0$ for $k = 1, 2, \cdots, p$, and $E\{w_i(n)w_k^*(n)\} = \sigma^2\delta_{i,k}$ and $E\{w_i(n)w_k(n)\} = 0$, where $E\{\cdot\}$ and $\delta_{i,k}$ denote the expectation and Kronecker delta.

Then, the calculation in Appendix B results in the following variance for the peak position error in terms of noise variance, signal power, and subarray size

$$\text{var}(\hat{\omega}_k) \approx \begin{cases} \dfrac{2(2m-1)\sigma^2}{3m(m-1)L^2|\beta_k|^2 r_s}, & \text{for } m \leq (M+1)/2 \\ \dfrac{2\sigma^2}{m(m-1)L|\beta_k|^2 r_s} \\ \cdot\left(1 - \dfrac{L(L-1)}{m(m-1)} \right. \\ \qquad \left. + \dfrac{(L-1)(2L-1)}{3m(m-1)}\right), & \text{for } m \geq (M+1)/2 \end{cases} \tag{22}$$

where ω_k denotes the "spatial frequency" $\omega_0\tau_k(\theta)$ for convenience, and r_s is the autocorrelation of the signal $s_1(n)$ given by $r_s = E\{s_1(n)s_1^*(n)\}$. Therefore, we can find that var$(\hat{\omega}_k)$ increases with subarray size m for $m \geq (M+1)/2$, whereas var$(\hat{\omega}_k)$ has the minimum when m is about $M/3+1$ for $m \leq (M+1)/2$. It is straightforward to show that the minimum variance of ω_k (and, hence, θ_k) can be obtained when the subarray size m is about $M/3+1$. The derivation and result for the FBLP-based method are similar and are omitted here.

We note that for two closely spaced coherent signals with equal power, a remarkable rule for the SS-based MUSIC scheme is that $m_{\text{opt}} = 0.6(M+1)$, which was derived by maximizing the distance between the signal and noise subspaces [42].

IV. Numerical Examples

The effectiveness of the proposed cyclic FBLP-based direction estimation approach is illustrated through several numerical examples, in which the desired coherent binary phase-shift keying (BPSK) signals can be distinguished from the interfering BPSK signals that have different cycle frequencies. In the simulations, the sensor separation of the ULA is $d = c/(2f_c)$, where the center frequency and speed of propagation are $f_c = 8$ MHz and $c = 3 \times 10^6$ m/s, respectively, the sensor outputs are collected at the rate $f_s = 8$ MHz, and the lag parameter Q is chosen as $Q = 10$. The BPSK signals have a raised-cosine pulse shape with 50% excess bandwidth. The additive noises are temporally and spatially uncorrelated white complex Gaussian noise with zero-mean and variance σ^2. The SNR is defined as the ratio of the power of the source signals to that of the additive noise at each sensor. For comparing the estimation performance, SS-based MUSIC [8], smoothed LP method [11], SS-based cyclic MUSIC [23], [50] and MODE (with linear constraint) [6], [47], are performed, and the Cramér–Rao lower bound (CRLB) [5] is calculated. For improving the estimation accuracy, the last step of the two-step procedure of the MODE algorithm is iterated five times (see [47] for more details). The results shown below are all based on 100 independent trials, and the dimension of signal subspace is assumed to be the number of desired coherent signals for the SS-based MUSIC and smoothed LP method.

Example 1—Performance versus SNR: We assess the performance of the proposed approach with respect to the SNR of the coherent signals. The direct-path signal from the BPSK 1 source impinges on the ULA of $M = 8$ sensors from angle $\theta_1 = -10°$ with 1.6 MHz baud rate ($\alpha = 0.2$ normalized to the sampling rate [17]), whereas one coherent arrival comes from $\theta_2 = 4°$ with mutipath coefficient $\beta_2 = 1$. There is one interfering BPSK 2 signal that arrives from $\theta_3 = 0°$ with 2.0 MHz baud rate ($\alpha = 0.25$ normalized to the sampling rate). Here, the numbers of impinging signals and coherent signals are $p = 3$ and $q = 2$. The number of snapshots and the subarray size are $N = 512$ and $m = 5$, where the number of subarrays is $2L = 8$. The SNR of the direct-path signal from the desired coherent source is varied from -5 dB to 30 dB, whereas that of the interference is fixed at 10 dB.

The root mean-squared-errors (RMSEs) of the estimates $\hat{\theta}_1$ and $\hat{\theta}_2$ versus SNR are shown in Fig. 1. Because SS-based MUSIC and smoothed LP method do not exploit the temporal properties of the incoming signals, they have no signal selective capability. Thus, they are unable to distinguish the desired signals from the interference correctly even when the dimension of signal subspace is assumed to be the number of coherent signals. Although the RMSE of estimate $\hat{\theta}_2$ obtained by MODE decreases as the SNR increases, the performance of MODE degrades severely at low SNR, and the estimate $\hat{\theta}_1$ has a rather large RMSE. Except at very low SNR, the proposed approach performs better over SS-based MUSIC and smoothed LP method, and the proposed approach is more accurate than SS-based cyclic MUSIC with its RMSE very close to the CRLB at higher SNR. We also find that the performance of the proposed approach is better than that of MODE at relatively low SNR.

Example 2—Performance versus Number of Snapshots: We examine the performance of the proposed approach in terms of the number of snapshots, where the simulation conditions are similar to those in Example 1, except that we fix the SNR of the direct-path signal at 10 dB and vary the number of snapshots N from 32 to 1024. Fig. 2 shows the RMSEs of the estimates $\hat{\theta}_1$ and $\hat{\theta}_2$ versus number of snapshots N. As described in Example 1, SS-based MUSIC and smoothed LP method fail to estimate the directions of the desired coherent signals correctly, and MODE performs worse as the number of data is not sufficiently large. When the length of the data is small, SS-based cyclic MUSIC degrades. However, the proposed approach outperforms SS-based MUSIC, the smoothed LP method, SS-based cyclic MUSIC, and MODE, and it can estimate the directions of coherent signals accurately even for a small number of snapshots. As the number of snapshots is increased, the improvement of the proposed approach is much larger than that of the other methods, although its asymptotic inefficiency is noticeable due to the finite length of data like the minimum norm LP method [24], [26], [35].

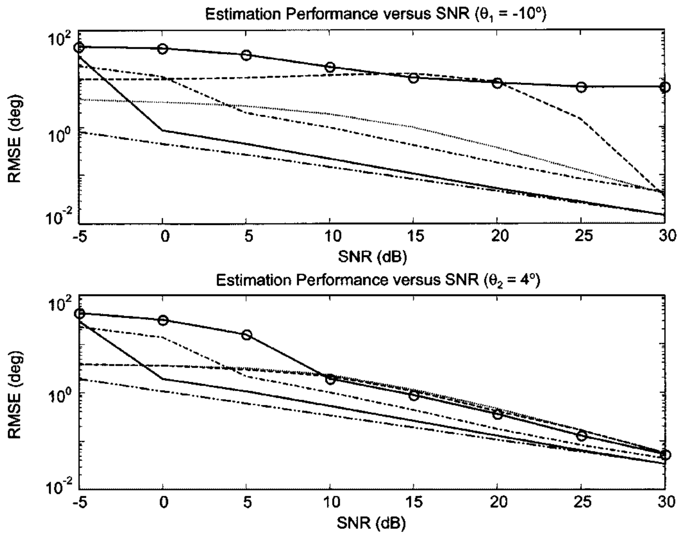

Fig. 1. RMSEs of the estimates of θ_1 and θ_2 versus SNR by using SS-based MUSIC (dotted line), smoothed LP (dashed line), SS-based cyclic MUSIC (dash–dot line), MODE (solid line with small circles) , and the proposed approach (solid line) in Example 1 (dash–dots line denotes CRLB).

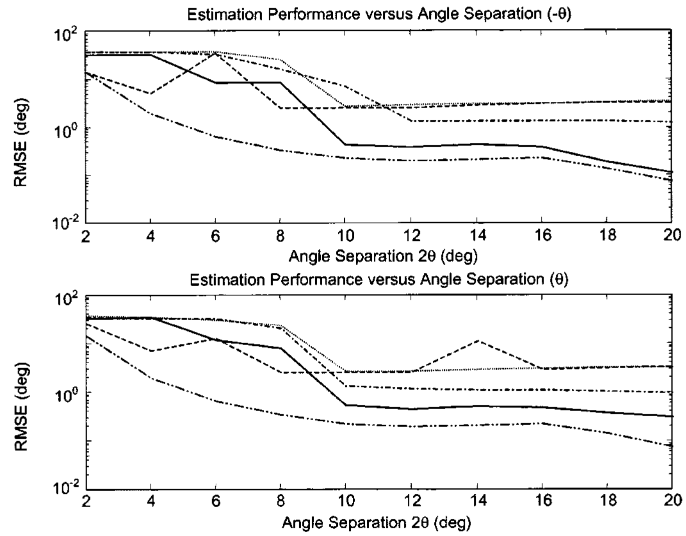

Fig. 3. RMSEs of the estimates of $\pm\theta$ versus angle separation 2θ by using SS-based MUSIC (dotted line), smoothed LP (dashed line), SS-based cyclic MUSIC (dash–dot line), and the proposed approach (solid line) in Example 3 (dash–dots line denotes CRLB).

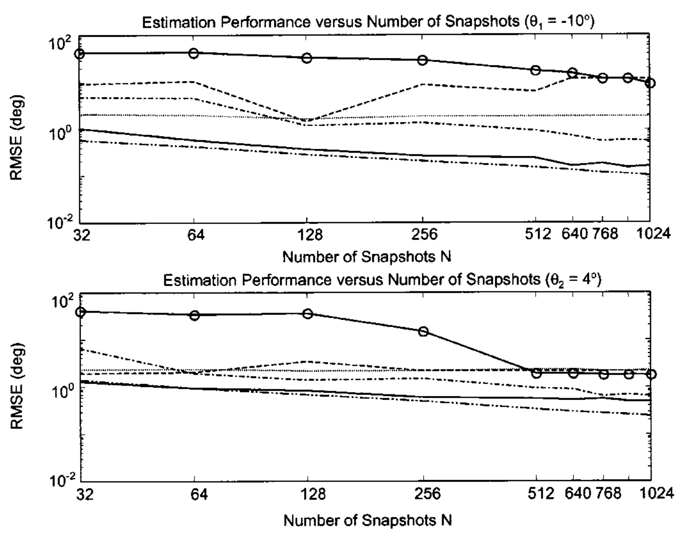

Fig. 2. RMSEs of the estimates of θ_1 and θ_2 versus number of snapshots by using SS-based MUSIC (dotted line), smoothed LP (dashed line), SS-based cyclic MUSIC (dash–dot line), MODE (solid line with small circles), and the proposed approach (solid line) in Example 2 (dash–dots line denotes CRLB).

Example 3—Performance versus Angle Separations: Here, we test the accuracy of the proposed approach against the angle separation between the desired coherent signals. The simulation parameters are identical to those in Example 1, except that the two coherent signals of BPSK 1 source come from $\pm\theta$ with equal power, where the SNR is fixed at 10 dB, and θ is varied from 1° to 10°. The RMSEs of the arrival angle estimates versus angle separation 2θ are plotted in Fig. 3. The simulation results show that the proposed approach can resolve the closely spaced coherent signals with much less RMSE than SS-based MUSIC, the smoothed LP method, and SS-based cyclic MUSIC in general. However, it is noted that the smoothed LP method gives better estimates with less RMSE for small angle separations in this empirical scenario.

Example 4—Performance versus Subarray Size: We study the effect of the subarray size (i.e., the order of the prediction model plus one) on the estimation performance of the proposed approach. The simulation parameters are the same as that in Example 1, except that the subarray size m is varied from 3 to 8, i.e., the number of subarrays is $2L = 12$ to 2.

For measuring the overall performance of estimating the directions of coherent signals in terms of the subarray size, we define an "empirical RMSE (ERMSE)" of the estimated directions as

$$\text{ERMSE} = \sqrt{\frac{1}{qK}\sum_{i=1}^{q}\sum_{k=1}^{K}\left(\hat{\theta}_i^{(k)} - \theta_i\right)^2} \tag{23}$$

where K is the number of trials, and $\hat{\theta}_i^{(k)}$ is the estimate obtained in the kth trial. When the SNR of the direct-path signal is -2.5 dB, 0 dB, 5 dB, and 17.5 dB, the ERMSEs of the estimates $\hat{\theta}_1$ and $\hat{\theta}_2$ against subarray size are shown in Fig. 4, where the "empirical CRLB" is calculated by averaging the corresponding CRLBs over the number of coherent signals. It is noted that the choice of subarray size m can significantly improve the performance of the proposed approach. We find that the best estimation can usually be attained when m is about $M/3+1$ for medium and high SNR, whereas a reasonable estimation can be obtained with a larger value of m for low SNR. The simulation results agree with the discussion in Section III; therefore, a compromise value of subarray size should be determined by balancing the effects of resolution and stability. We experimentally choose it to be approximately $M/3+1$ for high SNR [33], [39], [40].

Example 5—Performance versus Number of Sensors: Next, we consider the impact of the number of sensors on the estimation performance of the proposed approach. The simulation conditions are similar to that of Example 1, except that the SNR of direct-path signal is assumed be 10 dB, and the sensor number is varied as $M = 6$, 8, 10, 12, 16, 20 and 24, where the subarray size is chosen as $m = \text{round}(M/3) + 1$, where round denotes round-off operation. The RMSEs of the estimates $\hat{\theta}_1$

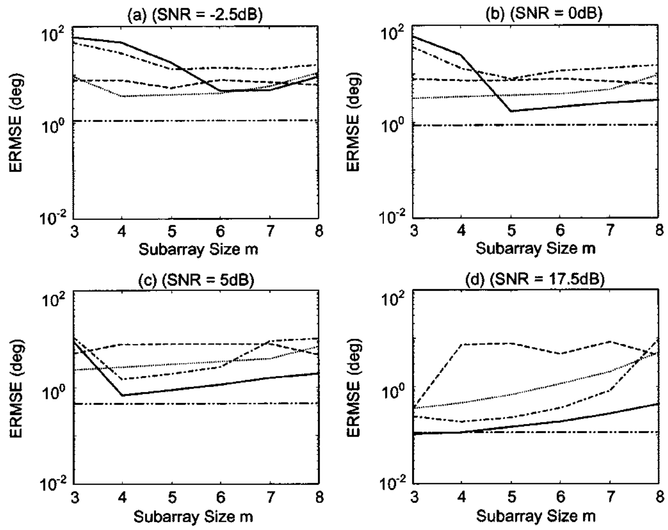

Fig. 4. ERMSE's of the estimates of θ_1 and θ_2 versus subarray size by using SS-based MUSIC (dotted line), smoothed LP (dashed line), SS-based cyclic MUSIC (dash–dot line), and the proposed approach (solid line) in Example 4 (dash–dots line denotes the empirical CRLB).

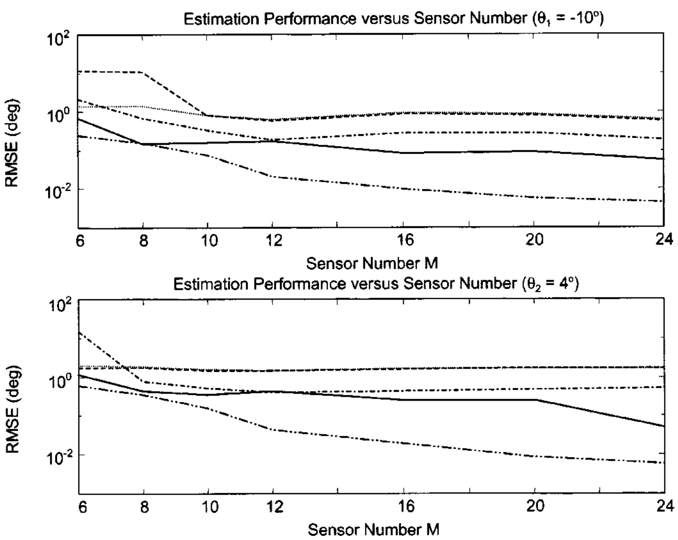

Fig. 5. RMSEs of the estimates of θ_1 and θ_2 versus number of sensors by using SS-based MUSIC (dotted line), smoothed LP (dashed line), SS-based cyclic MUSIC (dash–dot line), and the proposed approach (solid line) in Example 5 (dash–dots line denotes CRLB).

and $\hat{\theta}_2$ versus number of sensors are plotted in Fig. 5. As in the previous examples, the proposed approach outperforms SS-based MUSIC, the smoothed LP method, and SS-based cyclic MUSIC, and its superiority over the other methods improves as the number of sensors is increased.

Example 6—Performance of Signal Selective Capability: We verify the signal selective capability of the proposed cyclic FBLP-based approach to estimate the DOA of coherent signals from two sources with different cycle frequencies. Two coherent signals with equal power from the BPSK 1 source impinge on an array of $M = 10$ sensors from $\theta_1 = -2.5°$ and $\theta_2 = 9°$, whereas three coherent signals with equal power from the BPSK 2 source arrive from $\theta_3 = -13°$, $\theta_4 = 4°$, and $\theta_5 = 15°$. The SNR for each signal is 10 dB, the number of snapshots is $N = 512$, and the subarray size is chosen as $m = 5$.

We perform the proposed approach with $\alpha = 0.2$ and 0.25 to estimate the directions of the coherent signals from the two cyclostationary sources. Due to the presence of two coherent sources, the SS-based MUSIC and smoothed LP method cannot distinguish the desired coherent signals from the interfering signals even though the dimension of signal subspace is assumed to be $q = 2$ and $q = 3$, respectively, because they have no signal selective capability. To compare SS-based cyclic MUSIC and the proposed approach, the averaged estimate and the RMSE for each angle estimate are illustrated in Table I. Because the incoming signals are spatially close, SS-based cyclic MUSIC gives estimates with larger errors. However, the proposed approach can estimate the DOA of the two coherent sources more accurately.

V. Conclusions

Recently, many cyclostationarity-based direction estimation methods have been proposed for improving signal detection capability. Unfortunately, most of them perform as poorly as the ordinary subspace-based methods in multipath propagation scenarios, which are often encountered in many communications systems. To estimate the directions of narrowband coherent cyclostationary signals impinging on a ULA, we proposed a new cyclic approach by applying the LP technique. In order to improve the estimation performance, multiple lag parameters are used to exploit the cyclic statistics sufficiently and effectively. Moreover, the optimal subarray size that minimizes the peak position variance was derived using linear approximation for sufficiently high SNR. Since the computation of the cyclic array convariance matrix is avoided, the proposed approach has advantages over SS-based cyclic MUSIC in computation load and implementation. The effectiveness of the proposed approach was verified and compared with SS-based MUSIC, smoothed LP method, SS-based cyclic MUSIC, and MODE through numerical examples, and it was clarified that the proposed approach is superior in resolving the closely spaced coherent signals with a small number of snapshots and at low SNR.

Appendix A
Proof of Proposition

By defining $\boldsymbol{A}_1$ and $\boldsymbol{A}_2$ as the $(m-1)\times p$ and $L \times p$ submatrices of the $M \times p$ array steering matrix $\boldsymbol{A}$ in (3) consisting of the first $m-1$ and L rows, respectively, the noiseless signal vectors $\boldsymbol{x}_{f,l}(n)$ and $\boldsymbol{x}_{b,l}(n)$ in (5) and (6) can be expressed compactly [8], [34]

$$\boldsymbol{x}_{f,l}(n) = \boldsymbol{A}_1\boldsymbol{D}^{l-1}\boldsymbol{s}(n) \tag{A1}$$

$$\boldsymbol{x}_{b,l}(n) = \boldsymbol{A}_1\boldsymbol{D}^{l-1}(\boldsymbol{D}^{M-1}\boldsymbol{s}(n))^* \tag{A2}$$

where $\boldsymbol{D} = \mathrm{diag}(e^{j\omega_0\tau_1(\theta)}, e^{j\omega_0\tau_2(\theta)}, \cdots, e^{j\omega_0\tau_p(\theta)})$. From (1), (9), (11), and (A1), under the assumptions on the data model, we can rewrite the cyclic correlation vector $\boldsymbol{\varphi}_{f,l}(\tau)$ in (13) as

$$\begin{aligned}\boldsymbol{\varphi}_{f,l}^T(\tau) &= \langle \boldsymbol{y}_{f,l}^T(n)y_M^*(n+\tau)e^{-j2\pi\alpha n}\rangle \\ &= \boldsymbol{b}_M^H(\theta)\boldsymbol{\beta}^*\langle s_1^*(n+\tau)s_1(n)e^{-j2\pi\alpha n}\rangle\boldsymbol{\beta}^T\boldsymbol{D}^{l-1}\boldsymbol{A}_1^T \\ &= r_s^\alpha(\tau)\rho_M^*\boldsymbol{\beta}^T\boldsymbol{D}^{l-1}\boldsymbol{A}_1^T\end{aligned} \tag{A3}$$

TABLE I
COMPARISON OF THE AVERAGED ESTIMATES AND THE RMSES FOR EACH ANGLE ESTIMATE BY USING SS-BASED CYCLIC MUSIC AND THE PROPOSED CYCLIC FBLP-BASED APPROACH IN EXAMPLE 6

		$\theta_1 = -2.5°$	$\theta_2 = 9°$	$\theta_3 = -13°$	$\theta_4 = 4°$	$\theta_5 = 15°$
mean	SS cyclic MUSIC	-3.8712	8.4795	-12.8513	3.2666	14.8494
	proposed method	-2.9898	9.0442	-13.0865	4.5863	14.8529
RMSE	SS cyclic MUSIC	1.4205	0.6094	0.3634	1.1905	0.6453
	proposed method	0.5251	0.1609	0.1238	0.6338	0.2334

where $\rho_i = \boldsymbol{b}_i^T(\theta)\boldsymbol{\beta}$. Then, by some manipulations, we can re-expresse the cyclic matrix $\boldsymbol{\Phi}_f(\tau)$ in (15) as

$$\begin{aligned}\boldsymbol{\Phi}_f(\tau) =& r_s^\alpha(\tau)\rho_M^* \begin{bmatrix} \boldsymbol{\beta}^T\boldsymbol{A}_1^T \\ \boldsymbol{\beta}^T\boldsymbol{D}\boldsymbol{A}_1^T \\ \vdots \\ \boldsymbol{\beta}^T\boldsymbol{D}^{L-1}\boldsymbol{A}_1^T \end{bmatrix} \\ =& r_s^\alpha(\tau)\rho_M^*\boldsymbol{A}_2\boldsymbol{B}\boldsymbol{A}_1^T \end{aligned} \quad \text{(A4)}$$

where $\boldsymbol{B} = \text{diag}(\beta_1, \cdots \beta_q, \beta_{q+1}, \cdots, \beta_p)$. Equivalently, we have

$$\begin{aligned}\boldsymbol{\varphi}_{b,\,l}^T(\tau) =& \langle y_1(n)\boldsymbol{y}_{b,\,l}^T(n+\tau)e^{-j2\pi\alpha n}\rangle \\ =& r_s^\alpha(\tau)\rho_1\boldsymbol{\beta}^H\boldsymbol{D}^{-(M-1)}\boldsymbol{D}^{l-1}\boldsymbol{A}_1^T \quad \text{(A5)} \\ \boldsymbol{\Phi}_b(\tau) =& r_s^\alpha(\tau)\rho_1\boldsymbol{A}_2\boldsymbol{B}^*\boldsymbol{D}^{-(M-1)}\boldsymbol{A}_1^T. \quad \text{(A6)}\end{aligned}$$

By substituting (A4) and (A6) into the definition of the cyclic matrix $\boldsymbol{\Phi}(\tau)$ in (15), some straightforward manipulations give us

$$\begin{aligned}\boldsymbol{\Phi}(\tau) =& r_s^\alpha(\tau)\rho_M^* \begin{bmatrix} \boldsymbol{A}_2\boldsymbol{B} \\ \rho_1\boldsymbol{A}_2\boldsymbol{B}^*\boldsymbol{D}^{-(M-1)}/\rho_M^* \end{bmatrix} \boldsymbol{A}_1^T \\ =& r_s^\alpha(\tau)\rho_M^* \begin{bmatrix} \boldsymbol{A}_2\boldsymbol{B} \\ \boldsymbol{A}_2\boldsymbol{\Gamma}\boldsymbol{B} \end{bmatrix} \boldsymbol{A}_1^T \\ =& r_s^\alpha(\tau)\rho_M^*\boldsymbol{C}\boldsymbol{B}\boldsymbol{A}_1^T \end{aligned} \quad \text{(A7)}$$

where $\boldsymbol{\Gamma} = \text{diag}(\gamma_1, \cdots, \gamma_q, \gamma_{q+1}, \cdots, \gamma_p)$ with $\gamma_i = (\rho_1 \beta_i^*/\rho_M^*\beta_i)e^{-j\omega_0(M-1)\tau_i(\theta)}$ for $i = 1, 2, \cdots, q$, $\gamma_i = 0$ for $i = q+1, \cdots, p$, and $\boldsymbol{C} = [\boldsymbol{A}_2^T, (\boldsymbol{A}_2\boldsymbol{\Gamma})^T]^T$.

Because $\beta_k \neq 0$ for $k = 1, 2, \cdots, q$, whereas $\beta_k = 0$ for $k = q+1, \cdots, p$, the ranks of the matrices $\boldsymbol{B}$ and $\boldsymbol{\Gamma}$ are given by rank$(\boldsymbol{B})$ = rank$(\boldsymbol{\Gamma}) = q$. As $\boldsymbol{A}_1$ and $\boldsymbol{A}_2$ are the submatrices of the Vandermonde matrix $\boldsymbol{A}$, we clearly have rank$(\boldsymbol{A}_1) = \min(m-1, p)$ and rank$(\boldsymbol{A}_2) = \min(L, p)$. Consequently, since it has been assumed that $m \geq q+1$ and $q \leq p$, we obtain that rank$(\boldsymbol{A}_1) \geq q$. Additionally, the rank of the matrix $\boldsymbol{C}$ is given by rank$(\boldsymbol{C}) = \min(2L, p)$; therefore, rank$(\boldsymbol{C}) = q$ iff $2L \geq q$. Thus, if $2L \geq q$, the rank of the cyclic matrix $\boldsymbol{\Phi}(\tau)$ is equal to the number of the desired signals q regardless of the coherence of the source signals. Here, $\rho_M \neq 0$ and the assumption $r_s^\alpha(\tau) \neq 0$ are used implicitly. ■

APPENDIX B
DERIVATION OF VARIANCE OF SPECTRAL PEAK POSITION

By defining the correlation of noiseless signals $x_i(n)$ and $x_k(n)$ as $r_x(i-k) = E\{x_i(n)x_k^*(n)\}$, from (5), we can obtain the following relation between the LP parameters and the correlations:

$$r_x(k) = \sum_{i=1}^{m-1} r_x(k-i)a_i \quad \text{(B1)}$$

for $k = 1, 2, \cdots, m-1$, where $m-1 \geq p$. Then, the parameters $\{a_i\}$ can be determined by solving the $m-1$ Yule–Walker equations. In fact, the LP parameters $\{a_i\}$ satisfy the relation [43], [44]

$$a_i = \frac{1}{m-1}\sum_{k=1}^{p} \eta_k e^{j\omega_k i} \quad \text{(B2)}$$

where η_k is a complex constant. From (B1) and (B2), by some manipulations, we can succinctly express the Yule–Walker equations as $\boldsymbol{\Sigma}\boldsymbol{a} = \boldsymbol{g}$, where $\boldsymbol{\Sigma} = r_s\boldsymbol{A}_1^*\overline{\boldsymbol{B}}\boldsymbol{A}_1^T$, $\boldsymbol{g} = r_s\boldsymbol{A}_1^*\overline{\boldsymbol{B}}\boldsymbol{h}$, $\boldsymbol{a} = \boldsymbol{A}_1^*\overline{\boldsymbol{\eta}}/(m-1)$, $\overline{\boldsymbol{B}} = \boldsymbol{B}^*\boldsymbol{A}_2^H\boldsymbol{A}_2\boldsymbol{B}$, $\boldsymbol{h} = [e^{j(m-1)\omega_1}, e^{j(m-1)\omega_2}, \cdots, e^{j(m-1)\omega_p}]^T$, and $\overline{\boldsymbol{\eta}} = [\eta_1 e^{j(m-1)\omega_1}, \eta_2 e^{j(m-1)\omega_2}, \cdots, \eta_p e^{j(m-1)\omega_p}]^T$. After some manipulations, we can explicitly express the equations that needed to be solved as [43]

$$\eta_k + \sum_{\substack{i=1 \\ i\neq k}}^{p} \mu_{ki}\eta_i = 1 \quad \text{(B3)}$$

for $k = 1, 2, \cdots, p$, where $\mu_{ki} = e^{-j0.5m(\omega_k-\omega_i)}\sin(0.5(m-1)(\omega_k-\omega_i))/(m-1)\sin(0.5(\omega_k-\omega_i))$. Thus, the analytical expression of LP parameters $\{a_i\}$ can be obtained by solving a smaller set of p equations in the η_k coefficients, and then, the null-spectrum function $F_0(\omega) = |D_0(\omega)|^2$ can be exactly obtained, where $D_0(\omega) = \overline{\boldsymbol{a}}^H(\omega)\overline{\boldsymbol{a}}$, $\overline{\boldsymbol{a}}(\omega) = [1, e^{j\omega}, \cdots, e^{j(m-1)\omega}]^T$, and $\overline{\boldsymbol{a}} = [1, -a_1, \cdots, -a_{m-1}]^T$.

When there is additive noise, the estimates $\{\hat{a}_i\}$ can be expressed as $\hat{a}_i = a_i + \Delta a_i$, where Δa_i is the error, and the corresponding null-spectrum function can be written as $F(\omega) = |D(\omega)|^2$, where $D(\omega) = \overline{\boldsymbol{a}}^H(\omega)\hat{\overline{\boldsymbol{a}}}$, $\hat{\overline{\boldsymbol{a}}} = [1, -\hat{a}_1, \cdots, -\hat{a}_{m-1}]^T$, and the peak positions are related to the perturbation $D_1(\omega) = \overline{\boldsymbol{a}}^H(\omega)\Delta\overline{\boldsymbol{a}}$, where $\Delta\overline{\boldsymbol{a}} = [0, -\Delta\hat{a}_1, \cdots, -\Delta\hat{a}_{m-1}]^T$. Then, for the function $F(\omega)$ around the spatial frequency ω_k, we have the following Taylor series expansion for sufficiently large N:

$$F(\hat{\omega}_k) \approx F(\omega_k) + F'(\omega_k)(\hat{\omega}_k - \omega_k) \quad \text{(B4)}$$

$$0 = F'(\hat{\omega}_k) \approx F'(\omega_k) + F''(\omega_k)(\hat{\omega}_k - \omega_k) \quad \text{(B5)}$$

where $F'(\omega) = dF(\omega)/d\omega$ and $F''(\omega) = dF'(\omega)/d\omega$, and the higher-order derivative terms are neglected. Thus, the estimation error $\Delta\omega_k$ of the spatial frequency ω_k is given approximately by [5], [45]

$$\begin{aligned}\Delta\omega_k &= \hat{\omega}_k - \omega_k \approx -\frac{F'(\omega_k)}{F''(\omega_k)}\\ &= -\frac{\text{Re}\left\{\overline{\boldsymbol{a}}^H(\omega_k)\hat{\overline{\boldsymbol{a}}}\hat{\overline{\boldsymbol{a}}}^H\boldsymbol{d}(\omega_k)\right\}}{\text{Re}\left\{\boldsymbol{d}^H(\omega_k)\hat{\overline{\boldsymbol{a}}}\hat{\overline{\boldsymbol{a}}}^H\boldsymbol{d}(\omega_k)+\overline{\boldsymbol{a}}^H(\omega_k)\hat{\overline{\boldsymbol{a}}}\hat{\overline{\boldsymbol{a}}}^H\tilde{\boldsymbol{d}}(\omega_k)\right\}}\\ &\approx -\frac{\text{Re}\{D_1(\omega_k)\overline{\boldsymbol{a}}^H\boldsymbol{d}(\omega_k)\}}{\boldsymbol{d}^H(\omega_k)\overline{\boldsymbol{a}}\,\overline{\boldsymbol{a}}^H\boldsymbol{d}(\omega_k)}\end{aligned}\tag{B6}$$

where $\boldsymbol{d}(\omega) = d\overline{\boldsymbol{a}}(\omega)/d\omega$, and $\tilde{\boldsymbol{d}}(\omega) = d\boldsymbol{d}(\omega)/d\omega$ (the terms neglected in approximation are $O(1/N)$).

From (7), we get the following forward prediction error $e_{f,l}(n)$ for the estimate $\{\hat{a}_i\}$

$$\begin{aligned}e_{f,l}(n) &= y_{l+m-1}(n) - \boldsymbol{y}_{f,l}^T(n)\hat{\boldsymbol{a}}\\ &= s_1(n)\boldsymbol{\beta}^T\boldsymbol{D}^{l+m-2}\overline{\boldsymbol{A}}^H\Delta\overline{\boldsymbol{a}} + \overline{\boldsymbol{w}}_{f,l}^T(n)\hat{\overline{\boldsymbol{a}}}\end{aligned}\tag{B7}$$

where $\overline{\boldsymbol{A}} = [\overline{\boldsymbol{a}}(\omega_1), \overline{\boldsymbol{a}}(\omega_2), \cdots, \overline{\boldsymbol{a}}(\omega_p)]$, $\overline{\boldsymbol{w}}_{f,l}(n) = [w_{l+m-1}(n), w_{l+m-2}(n), \cdots, w_l(n)]^T$, and $D_0(\omega_k) = \overline{\boldsymbol{a}}^H(\omega_k)\overline{\boldsymbol{a}} = 0$ is used implicitly. Then, we obtain the prediction error power $e(n)$

$$\begin{aligned}e(n) &= \frac{1}{L}\sum_{l=1}^{L}|e_{f,l}(n)|^2\\ &\approx \frac{1}{L}\Big\{s_1^*(n)s_1(n)\boldsymbol{\psi}^H(\omega)\boldsymbol{B}^*\boldsymbol{D}^{-(m-1)}\boldsymbol{A}_2^H\\ &\quad\cdot \boldsymbol{A}_2\boldsymbol{D}^{m-1}\boldsymbol{B}\boldsymbol{\psi}(\omega) + 2\\ &\quad\cdot \text{Re}\left\{s_1^*(n)\boldsymbol{\psi}^H(\omega)\boldsymbol{B}^*\boldsymbol{D}^{-(m-1)}\boldsymbol{A}_2^H\boldsymbol{W}_f(n)\overline{\boldsymbol{a}}\right\}\\ &\quad + \overline{\boldsymbol{a}}^H\boldsymbol{W}_f^H(n)\boldsymbol{W}_f(n)\overline{\boldsymbol{a}}\Big\}\end{aligned}\tag{B8}$$

where $\boldsymbol{\psi}(\omega) = \overline{\boldsymbol{A}}^H\Delta\overline{\boldsymbol{a}} = [D_1(\omega_1), D_1(\omega_2), \cdots, D_1(\omega_p)]^T$, $\boldsymbol{W}_f(n) = [\overline{\boldsymbol{w}}_{f,1}(n), \overline{\boldsymbol{w}}_{f,2}(n), \cdots, \overline{\boldsymbol{w}}_{f,L}(n)]^T$, and the small terms are neglected in the approximation. By following the idea of [45], we can find the perturbation $D_1(\omega_k)$ by an approximate minimization of the prediction error power $e(n)$ in (B8). Letting the derivative of $e(n)$ with respect to $D_1(\omega_k)$ be zero, it follows that

$$\sum_{l=0}^{L-1}\boldsymbol{\xi}^T(\omega_k)\boldsymbol{\psi}(\omega) = -e^{-j(m-1)\omega_k}\boldsymbol{a}_2^H(\omega_k)\boldsymbol{W}_f(n)\overline{\boldsymbol{a}}\tag{B9}$$

for $k = 1, 2, \cdots, p$, where $\boldsymbol{\xi}(\omega_k) = [s_1(n)e^{j(l+m-1)(\omega_1-\omega_k)}, s_2(n)e^{j(l+m-1)(\omega_2-\omega_k)}, \cdots, s_p(n)e^{j(l+m-1)(\omega_p-\omega_k)}]^T$, and $\boldsymbol{a}_2(\omega_k) = [1, e^{j\omega_k}, \cdots, e^{j(L-1)\omega_k}]^T$.

Therefore, by solving the two $p \times p$ equations (B3) and (B9) to get $\{a_i\}$ and $D_1(\omega_k)$, we can obtain the approximate error $\Delta\omega_k$ of peak position ω_k from (B6). For obtaining a simple expression of the variance of spectral peak position, here, we consider the "well-separated" signals [i.e., $(m-1)|\omega_l - \omega_k| \gg 1$], where the two equations (B3) and (B9) can be approximated as diagonal. As a result, we obtain $\Delta\omega_k \approx -2\text{Im}\{D_1(\omega_k)\}/m$, where the LP parameters $\{a_i\}$ and $D_1(\omega_k)$ are given by

$$a_i = \frac{1}{m-1}\sum_{k=1}^{p}e^{j\omega_k i}\tag{B10}$$

$$D_1(\omega_k) = -\frac{1}{Ls_k(n)}e^{-j(m-1)\omega_k}\boldsymbol{a}_2^H(\omega_k)\boldsymbol{W}_f(n)\overline{\boldsymbol{a}}\tag{B11}$$

and $\boldsymbol{d}^H(\omega_k)\overline{\boldsymbol{a}} \approx jm/2$. For sufficiently large N, the variance of the estimate $\hat{\omega}_k$ is then given by

$$\text{var}(\hat{\omega}_k) \approx \frac{2}{m^2}(\text{Re}\{E\{|D_1(\omega_k)|^2\}\} - \text{Re}\{E\{D_1^2(\omega_k)\}\}).\tag{B12}$$

From the fact that for matrix $\boldsymbol{X}$ and vector $\boldsymbol{c}$ with compatible dimensions that $\boldsymbol{X}\boldsymbol{c} = (\boldsymbol{I}\otimes\boldsymbol{c}^T)\text{vec}(\boldsymbol{X}^T)$, where $\text{vec}(\boldsymbol{X}^T)$ is a vector obtained by listing the columns of $\boldsymbol{X}^T$ one beneath the other beginning with the leftmost column, and $\otimes$ denotes the Kronecker operation, we can get

$$E\{|D_1(\omega_k)|^2\} = \frac{1}{L^2 r_{s_k}}\boldsymbol{a}_2^H(\omega_k)\boldsymbol{\Sigma}\boldsymbol{a}_2(\omega_k)\tag{B13}$$

where $\boldsymbol{\Sigma} = (\boldsymbol{I}_L\otimes\overline{\boldsymbol{a}}^T)E\{\text{vec}(\boldsymbol{W}_f^T(n))\text{vec}^H(\boldsymbol{W}_f^T(n))\}(\boldsymbol{I}_L\otimes\overline{\boldsymbol{a}}^*)$, $\boldsymbol{I}_L$ is the $L\times L$ identity matrix, and $r_{s_k} = E\{s_k(n)s_k^*(n)\}$. By performing some manipulations, the ikth element of the matrix $\boldsymbol{\Sigma}$ is given by

$$\boldsymbol{\Sigma}_{ik} = \begin{cases}\sigma^2 m/(m-1), & \text{for } |i-k| = 0\\ -|i-k|\sigma^2 e^{j(i-k)\omega_k}/(m-1)^2, & \text{for } 0 < |i-k| \le m-1\\ 0, & \text{for } |i-k| > m-1\end{cases}\tag{B14}$$

where $i, k = 1, 2, \cdots, L$. From (B13) and (B14), we then have

$$\begin{aligned}&E\{|D_1(\omega_k)|^2\}\\ &\quad= \frac{\sigma^2}{L^2 r_{s_k}}\left(\frac{m}{m-1}L - \frac{2}{(m-1)^2}\sum_{k=1}^{m-1}k(L-k)\right)\\ &\quad= \frac{m(2m-1)\sigma^2}{3(m-1)L^2 r_{s_k}}\end{aligned}\tag{B15}$$

for $L \ge m$ [i.e., $m \le (M+1)/2$], and we get

$$\begin{aligned}&E\{|D_1(\omega_k)|^2\}\\ &\quad= \frac{\sigma^2}{L^2 r_{s_k}}\left(\frac{m}{m-1}L - \frac{2}{(m-1)^2}\sum_{k=1}^{L-1}k(L-k)\right)\\ &\quad= \frac{m\sigma^2}{(m-1)Lr_{s_k}}\left(1 - \frac{L(L-1)}{m(m-1)} + \frac{(L-1)(2L-1)}{3m(m-1)}\right)\end{aligned}\tag{B16}$$

for $L \leq m$ [i.e., $m \geq (M+1)/2$]. On the other hand, we have

$$E\{D_1^2(\omega_k)\} = 0 \tag{B17}$$

because $E\{w_i(n)w_k(n)\} = 0$. Thus, by substituting (B15)–(B17) into (B12), (22) can be obtained. ■

ACKNOWLEDGMENT

The authors would like to thank the anonymous reviewers and the associate editor Prof. J. Li for constructive comments and valuable suggestions that improved the manuscript. They are particularly grateful to the reviewer who brought [41] and [42] to their attention.

REFERENCES

[1] R. O. Schmidt, "Multiple emitter location and signal parameter estimation," *IEEE Trans. Antennas Propagat.*, vol. AP-34, pp. 276–280, Mar. 1986.
[2] R. Roy and T. Kailath, "ESPRIT—Estimation of signal parameters via rational invariance techniques," *IEEE Trans. Acoust., Speech, Signal Processing*, vol. 37, pp. 984–995, July 1989.
[3] R. Kumaresan and D. W. Tufts, "Estimating the angles of arrival of multiple plane waves," *IEEE Trans. Aerosp. Electron. Syst.*, vol. AES-19, pp. 134–139, Jan. 1983.
[4] I. Ziskind and M. Wax, "Maximum likelihood localization of multiple sources by alternating projection," *IEEE Trans. Acoust., Speech, Signal Processing*, vol. 36, pp. 1553–1560, Oct. 1988.
[5] P. Stoica and A. Nehorai, "MUSIC, maximum likelihood, and Cramer–Rao bound," *IEEE Trans. Acoust., Speech, Signal Processing*, vol. 37, pp. 720–741, May 1989.
[6] P. Stoica and K. C. Sharman, "Maximum likelihood methods for direction-of-arrival estimation," *IEEE Trans. Acoust., Speech, Signal Processing*, vol. 38, pp. 1132–1143, July 1990.
[7] J. Sheinvald, M. Wax, and A. J. Weiss, "On maximum-likelihood localization of coherent signals," *IEEE Trans. Signal Processing*, vol. 44, pp. 2475–2482, Oct. 1996.
[8] T. J. Shan, M. Wax, and T. Kailath, "On spatial smoothing for direction-of-arrival estimation of coherent signals," *IEEE Trans. Acoust., Speech, Signal Processing*, vol. ASSP-33, pp. 806–811, Apr. 1985.
[9] S. Haykin, "Radar array processing for angle of arrival estimation," in *Array Signal Processing*, S. Haykin, Ed. Englewood Cliffs, NJ: Prentice-Hall, 1985, pp. 194–292.
[10] J. A. Cadzow, "A high resolution direction-of-arrival algorithm for narrow-band coherent and incoherent sources," *IEEE Trans. Acoust., Speech, Signal Processing*, vol. 36, pp. 965–979, July 1988.
[11] H. Krim and J. G. Proakis, "Smoothed eigenspace-based parameter estimation," *Automatica*, vol. 30, no. 4, pp. 27–38, 1994.
[12] S. S. Reddi and A. B. Gershman, "An alternative approach to coherent source location problem," *Signal Process.*, vol. 59, no. 2, pp. 221–233, 1997.
[13] W. A. Gardner, "Exploitation of spectral redundancy in cyclostationary signals," *IEEE Signal Processing Mag.*, vol. 8, pp. 14–37, Apr. 1991.
[14] W. A. Gardner, Ed., *Cyclostationarity in Communications and Signal Processing*. Piscataway, NJ: IEEE, 1994.
[15] W. A. Gardner, "Simplification of MUSIC and ESPRIT by exploitation of cyclostationarity," *Proc. IEEE*, vol. 76, pp. 845–847, July 1988.
[16] L. Izzo, L. Paura, and G. Poggi, "An interference-tolerant algorithm for localization of cyclostationary-signal sources," *IEEE Trans. Signal Processing*, vol. 40, pp. 1682–1686, July 1991.
[17] G. Xu and T. Kailath, "Direction-of-arrival estimation via exploitation of cyclostationarity—A combination of temporal and spatial processing," *IEEE Trans. Signal Processing*, vol. 40, pp. 1775–1786, July 1992.
[18] S. V. Schell, "Performance analysis of the cyclic MUSIC method of direction estimation for cyclostationary signals," *IEEE Trans. Signal Processing*, vol. 40, pp. 3043–3050, Nov. 1992.
[19] G. Gelli and L. Izzo, "Minimum-redundancy linear arrays for cyclostationarity-based source location," *IEEE Trans. Signal Processing*, vol. 45, pp. 2605–2608, Oct. 1997.
[20] S. Shamsunder and G. B. Giannakis, "Signal selective localization of nonGaussian cyclostationary sources," *IEEE Trans. Signal Processing*, vol. 42, pp. 2860–2864, Oct. 1994.
[21] J. Xin, H. Tsuji, S. Yoshimoto, and A. Sano, "Minimum MSE-based detection of cyclostationary signals in array processing," in *Proc. IEEE First Signal Process. Workshop Signal Process. Adv. Wireless Commun.*, Paris, France, Apr. 1997, pp. 169–172.
[22] S. V. Schell and W. A. Gardner, "Signal-selective high-resolution direction finding in multipath," in *Proc. IEEE Int. Conf. Acoust., Speech, Signal Process.*, Albuquerque, NM, Apr. 1990, pp. 2667–2670.
[23] J. Xin, H. Tsuji, Y. Hase, and A. Sano, "Directions-of-arrival estimation of cyclostationary coherent signals in array processing," *IEICE Trans. Fund.*, vol. E81-A, no. 8, pp. 1560–1569, 1998.
[24] D. W. Tufts and R. Kumaresan, "Estimation of frequencies of multiple sinusoids: Making linear prediction perform like maximum likelihood," *Proc. IEEE*, vol. 70, pp. 975–989, Sept. 1982.
[25] D. H. Johnson, "The application of spectral estimation methods to bearing estimation problems," *Proc. IEEE*, vol. 70, pp. 1018–1028, Sept. 1982.
[26] M. Kaveh and A. J. Barabell, "The statistical performance of MUSIC and the minimum-norm algorithms in resolving plane waves in noise," *IEEE Trans. Acoust., Speech, Signal Process.*, vol. ASSP-34, pp. 331–341, Feb. 1986.
[27] P. Burns and Z. Ding, "Robustification of cyclostationary array processing techniques," in *Proc. IEEE Int. Conf. Acoust., Speech, Signal Process.*, Detroit, MI, May 1995, pp. 1589–1592.
[28] E. Gonen and J. M. Mendel, "Applications of cumulants to array processing—Part IV: Direction finding in coherent signals case," *IEEE Trans. Signal Processing*, vol. 45, pp. 2265–2276, Sept. 1997.
[29] A. V. Dandawate and G. B. Giannakis, "Statistical tests for presence of cyclostationarity," *IEEE Trans. Signal Processing*, vol. 42, pp. 2355–2369, Sept. 1994.
[30] S. L. Marple Jr., *Digital Spectral Analysis with Applications*. Englewood Cliffs, NJ: Prentice-Hall, 1987.
[31] B. D. Rao, "Perturbation analysis of an SVD-based linear prediction method for estimating the frequencies of multiple sinusoids," *IEEE Trans. Acoust., Speech, Signal Processing*, vol. 36, pp. 1026–1035, July 1988.
[32] T. Söderström, "Identification of stochastic linear systems in presence of input noise," *Automatica*, vol. 17, no. 5, pp. 713–725, 1981.
[33] M. A. Rahman and K.-B. Yu, "Total least squares approach for frequency estimation using linear prediction," *IEEE Trans. Acoust., Speech, Signal Processing*, vol. ASSP-35, pp. 1440–1454, Oct. 1987.
[34] S. U. Pillai and B. H. Kwon, "Forward/backward spatial smoothing techniques for coherent signals identification," *IEEE Trans. Acoust., Speech, Signal Processing*, vol. 37, pp. 8–15, Jan. 1989.
[35] D. W. Tufts and R. Kumaresan, "Singular value decomposition and improved frequency estimation using linear prediction," *IEEE Trans. Acoust., Speech, Signal Processing*, vol. 30, pp. 671–675, Apr. 1982.
[36] B. D. Rao and K. S. Arun, "Model based processing of signals: A state space approach," *Proc. IEEE*, vol. 80, pp. 283–309, Feb. 1992.
[37] W. Du and R. L. Kirlin, "Improved spatial smoothing techniques for DOA estimation of coherent signals," *IEEE Trans. Signal Processing*, vol. 39, pp. 1208–1210, May 1991.
[38] P. C. Hansen, "Truncated singular value decomposition solutions to discrete ill-posed problems with ill-determined numerical rank," *SIAM J. Sci. Stat. Comput.*, vol. 11, no. 3, pp. 503–518, 1990.
[39] W. M. Steedly, C. J. Ying, and R. L. Moses, "Statistical analysis of TLS-based Prony techniques," *Automatica*, vol. 30, no. 1, pp. 115–129, 1994.
[40] H. Clergeot, S. Tressens, and A. Ouamri, "Performance of high resolution frequencies estimation methods compared to the Cramer–Rao bounds," *IEEE Trans. Acoust., Speech, Signal Processing*, vol. 37, pp. 1703–1720, Nov. 1989.
[41] P. Stoica and K. C. Sharman, "Novel eigenanalysis method for direction estimation," *Proc. Inst. Elect. Eng. F*, vol. 137, no. 1, pp. 19–26, 1990.
[42] A. B. Gershman and V. T. Ermolaev, "Optimal subarray size for spatial smoothing," *IEEE Signal Processing Lett.*, vol. 2, pp. 28–30, Feb. 1995.
[43] S. M. Kay, *Modern Spectral Estimation: Theory and Application*. Englewood Cliffs, NJ: Prentice-Hall, 1987.
[44] E. H. Satorius and J. R. Zeidler, "Maximum entropy spectral analysis of multiple sinusoids in noise," *Geophysics*, vol. 43, no. 6, pp. 1111–1118, 1978.
[45] S. W. Lang and J. H. McClellan, "Frequency estimation with maximum entropy spectral estimators," *IEEE Trans. Acoust., Speech, Signal Processing*, vol. ASSP-28, pp. 716–724, June 1980.
[46] H. Kagiwada, Y. Aoki, J. Xin, and A. Sano, "Determination of number of signals based on minimum MSE," *IEICE Trans. Fund.*, vol. J80-A, no. 2, pp. 317–326, 1997.

[47] J. Li, P. Stoica, and Z.-S. Liu, "Comparative study of IQML and MODE direction-of-arrival estimators," *IEEE Trans. Signal Processing*, vol. 46, pp. 149–160, Jan. 1998.

[48] P. Stoica and M. Jansson, "On forward–backward MODE for array signal processing," *Digital Signal Process.*, vol. 7, pp. 239–252, 1997.

[49] A. B. Gershman and P. Stoica, "New MODE-based techniques for directions finding with an improved threshold performance," *Signal Process.*, vol. 76, pp. 221–235, 1999.

[50] J. Xin, H. Tsuji, Y. Hase, and A. Sano, "Directions-of-arrival estimation of cyclostationary coherent signals in array processing," in *Proc. IX Euro. Signal Process. Conf.*, vol. III, Rhodes, Greece, Sept. 1998, pp. 1781–1784.

Jingmin Xin (S'92–M'96) received the B.E. degree in information and control engineering from Xi'an Jiaotong University, Xi'an, China, in 1988 and the M.E. and Ph.D. degrees in electrical engineering from Keio University, Yokohama, Japan, in 1993 and 1996, respectively.

From 1988 to 1990, he was with the Tenth Institute of Ministry of Posts and Telecommunications (MPT) of China, Xi'an. He was with Communications Research Laboratory, MPT of Japan, as an Invited Research Fellow of Telecommunications Advancement Organization of Japan (TAO) from 1996 to 1997 and as a Postdoctoral Fellow of Japan Science and Technology Corporation (JST) from 1997 to 1999. Since 1999, he has been a Guest Researcher with YRP Mobile Telecommunications Key Technology Research Laboratories Co., Ltd., Yokosuka, Japan. His research interests are in the areas of digital signal processing, system identification, and their application to mobile communication systems.

Akira Sano (M'89) received the B.E., M.E., and Ph.D. degrees in mathematical engineering and information physics from the University of Tokyo, Tokyo, Japan, in 1966, 1968, and 1971, respectively.

He joined the Department of Electrical Engineering, Keio University, Yokohama, Japan, in 1971, and he is currently a Professor of the Department of System Design Engineering. He was a Visiting Research Fellow at the University of Salford, Salford, U.K., from 1977 to 1978. Since 1995, he has been a Visiting Research Fellow at the Communication Research Laboratory, Ministry of Posts and Telecommunications. His current research interests are in adaptive modeling and design theory in control, signal processing and communication, and applications to control of sounds and vibrations, mechanical systems, and mobile communication systems. He is a co-author of the textbook *State Variable Methods in Automatic Control* (New York: Wiley, 1988).

Dr. Sano received the Kelvin Premium from the Institute of Electrical Engineering in 1986. He is a Fellow of the Society of Instrument and Control Engineers and a member of the Institute of Electrical Engineering of Japan and the Institute of Electronics, Information, and Communications Engineers of Japan. He was General Co-chair of 1999 IEEE Conference of Control Applications and has served as Chair of the IFAC Technical Committee on Modeling and Control of Environmental Systems since 1996. He has also been Vice Chair of IFAC Technical Committee on Adaptive Control and Learning since 1999.